



Basaltic Rocks Analyzed by the Spirit Rover in Gusev Crater

H. Y. McSween, *et al.*
Science **305**, 842 (2004);
DOI: 10.1126/science.3050842

The following resources related to this article are available online at www.sciencemag.org (this information is current as of June 12, 2007):

Updated information and services, including high-resolution figures, can be found in the online version of this article at:

<http://www.sciencemag.org/cgi/content/full/305/5685/842>

Supporting Online Material can be found at:

<http://www.sciencemag.org/cgi/content/full/305/5685/842/DC1>

A list of selected additional articles on the Science Web sites **related to this article** can be found at:

<http://www.sciencemag.org/cgi/content/full/305/5685/842#related-content>

This article **cites 15 articles**, 10 of which can be accessed for free:

<http://www.sciencemag.org/cgi/content/full/305/5685/842#otherarticles>

This article has been **cited by** 71 article(s) on the ISI Web of Science.

This article has been **cited by** 16 articles hosted by HighWire Press; see:

<http://www.sciencemag.org/cgi/content/full/305/5685/842#otherarticles>

Information about obtaining **reprints** of this article or about obtaining **permission to reproduce this article** in whole or in part can be found at:

<http://www.sciencemag.org/about/permissions.dtl>

43. P. R. Christensen *et al.*, *J. Geophys. Res.* **106**, 23823 (2001).
44. H. H. Kieffer *et al.*, *J. Geophys. Res.* **82**, 4249 (1977).
45. M. T. Mellon, B. M. Jakosky, H. H. Kieffer, P. R. Christensen, *Icarus* **148**, 437 (2000).
46. R. L. Fergason, P. R. Christensen, *Proc. Lunar Planet. Sci.* **XXXIV**, abstr. 1785 (2003).
47. M. P. Golombek *et al.*, *Proc. Lunar Planet. Sci.* **XXXIV**, abstr. 25041 (2004).
48. H. H. Kieffer, J. S. C. Chase, E. Miner, G. Munch, G. Neugebauer, *J. Geophys. Res.* **78**, 4291 (1973).
49. M. A. Presley, P. R. Christensen, *J. Geophys. Res.* **102**, 6551 (1997).
50. K. S. Edgett, P. R. Christensen, *J. Geophys. Res.* **96**, 22,765 (1991).
51. M. P. Golombek *et al.*, *J. Geophys. Res.* **108**, 10.1029/2002JE0020235 (2003).
52. P. R. Christensen, *Icarus* **68**, 217 (1986).
53. M. P. Golombek *et al.*, *J. Geophys. Res.* **108**, 1029/2003JE002074 (2003).
54. We would like to express our deepest appreciation to all of the individuals at Raytheon Santa Barbara Remote Sensing, led by S. Silverman, and at the Jet Propulsion Laboratory whose effort and dedication have led to the successful acquisition of Mini-TES data from the surface at Gusev Crater. Funding was provided by the MER Project Science Office.

Supporting Online Material

www.sciencemag.org/cgi/content/full/305/5685/837/DC1

Materials and Methods

SOM Text

Fig. S1

Plates Referenced in Article

www.sciencemag.org/cgi/content/full/305/5685/837/DC2

Plate 6

21 May 2004; accepted 7 July 2004

REPORT

Basaltic Rocks Analyzed by the Spirit Rover in Gusev Crater

H. Y. McSween,¹ R. E. Arvidson,² J. F. Bell III,³ D. Blaney,⁴ N. A. Cabrol,⁵ P. R. Christensen,⁶ B. C. Clark,⁷ J. A. Crisp,⁴ L. S. Crumpler,⁸ D. J. Des Marais,⁵ J. D. Farmer,⁶ R. Gellert,⁹ A. Ghosh,¹ S. Gorevan,¹⁰ T. Graff,⁶ J. Grant,¹¹ L. A. Haskin,² K. E. Herkenhoff,¹² J. R. Johnson,¹² B. L. Jolliff,² G. Klingelhofer,¹³ A. T. Knudson,⁶ S. McLennan,¹⁴ K. A. Milam,¹ J. E. Moersch,¹ R. V. Morris,¹⁵ R. Rieder,⁹ S. W. Ruff,⁶ P. A. de Souza Jr.,¹⁶ S. W. Squyres,³ H. Wänke,⁹ A. Wang,² M. B. Wyatt,⁶ A. Yen,⁴ J. Zipfel⁹

The Spirit landing site in Gusev Crater on Mars contains dark, fine-grained, vesicular rocks interpreted as lavas. Pancam and Mini-Thermal Emission Spectrometer (Mini-TES) spectra suggest that all of these rocks are similar but have variable coatings and dust mantles. Magnified images of brushed and abraded rock surfaces show alteration rinds and veins. Rock interiors contain $\leq 25\%$ megacrysts. Chemical analyses of rocks by the Alpha Particle X-ray Spectrometer are consistent with picritic basalts, containing normative olivine, pyroxenes, plagioclase, and accessory FeTi oxides. Mössbauer, Pancam, and Mini-TES spectra confirm the presence of olivine, magnetite, and probably pyroxene. These basalts extend the known range of rock compositions composing the martian crust.

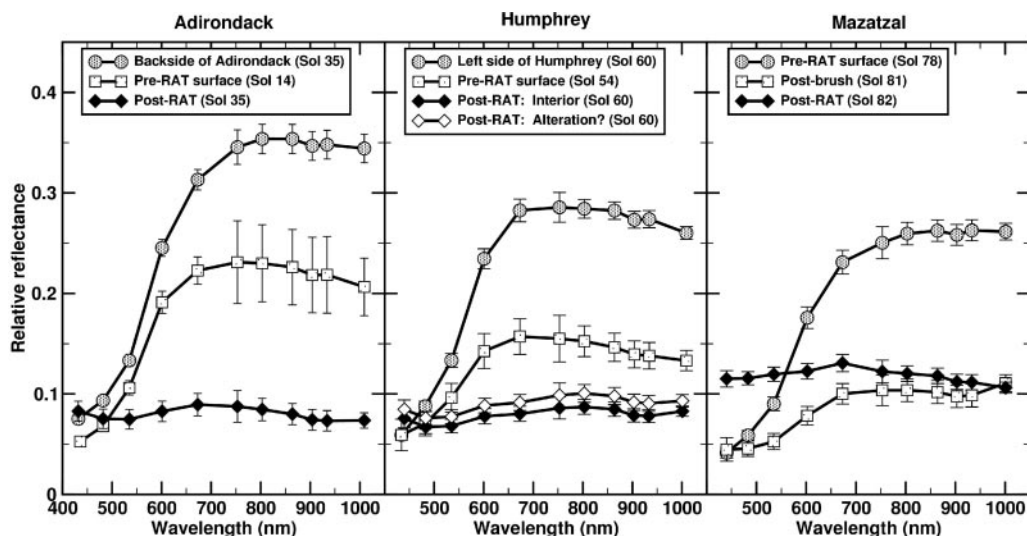
Rocks at the Spirit landing site are fine-grained with irregular vesicles and vugs, suggesting a volcanic origin. The rocks are angular and strewn across the surface, which suggests they were ejected from nearby Bonnevill crater (1) by an impact event (2).

Pancam and Mini-Thermal Emission Spectrometer (Mini-TES) spectra of rock surfaces indicate two end members, represented by dark- and light-toned rocks, with most rocks falling between these extremes. Three representative rocks, Adirondack, Humphrey,

and Mazatzal, located several hundred meters apart, have been analyzed with the Athena instruments (3). Pancam images (4) show that Adirondack and Humphrey are partly coated and that Mazatzal is uniformly coated by light-toned material (Plates 9A, 10A, and 11A). Pancam spectra (Fig. 1) of the dark portions of Adirondack and Humphrey are consistent with the presence of olivine, which has a broad (composite) absorption band near 1000 nm. A weak band center near 930 nm suggests the presence of pyroxene or contamination by ferric oxides.

The long-wavelength portion of Mini-TES spectra of dark rock surfaces resembles the Mars Global Surveyor (MGS)-TES spectra of

Fig. 1. Relative reflectance Pancam spectra of Adirondack, Humphrey, and Mazatzal (20). Dark-toned portions and abraded interiors (post-RAT) of rocks have flat, relatively featureless spectra consistent with basalt.



olivine-bearing basalts seen elsewhere on Mars (5). An emissivity peak at $\sim 450\text{ cm}^{-1}$ in the spectra of dark portions of Adirondack and Humphrey is consistent with intermediate olivine (Fo36–60), but an as-yet-unidentified feature at $\sim 875\text{ cm}^{-1}$ (also seen in orbital TES spectra of the Gusev landing site) complicates mineral deconvolution of these spectra (6).

Mini-TES spectra of the darkest portions of the rocks do not show any scattering at short thermal infrared wavelengths ($>1300\text{ cm}^{-1}$) that is characteristic of micrometer-size particles, suggesting that if a coating is present, it is either coherent or a thin ($<10\text{ }\mu\text{m}$) veneer of unconsolidated dust. A Microscopic Imager (MI) image of the surface of Humphrey reveals several hexagonal pits (Fig. 2), consistent with the shapes of olivine crystals. Only a coherent layer could retain mineral casts. The Rock Abrasion Tool (RAT) was used to brush and abrade rock surfaces (3), exposing dark, nearly dust-free

rocks (Plates 9B, 10B, 10C, 11B, 11C) with similar textures (Fig. 3). A smooth, dark coating, bounded above and below by thin white coatings (possibly cemented dust), was revealed in images of brushed and ground areas on Mazatzal (7). RAT abrasion of Humphrey created an oblique cut (8), and an MI image of the transition between the surface and rock interior displays a different texture (Fig. 2), interpreted as an alteration rind. Multiple, adjacent areas of Humphrey and Mazatzal were brushed to produce an area that would fill the Mini-TES field of view. The brushed Humphrey Mini-TES spectra were indistinguishable from the prebrushed rock spectra,

but the Mazatzal spectra of the prebrushed and brushed surfaces were distinct, consistent with the multiple coatings observed in MI images (6).

MI observations of the Adirondack and Mazatzal RAT holes revealed fractures filled with light-toned materials, along with dispersed patches of light-toned grains. The fracture in Mazatzal crosscuts the rock and its dark coating (Plate 11B). Humphrey contains a network of tiny, irregular light-toned veins (Figs. 2 and 3B). The absence of red coloration in high-resolution Pancam images of the fractures and veins (4) indicates that they are not filled with dust.

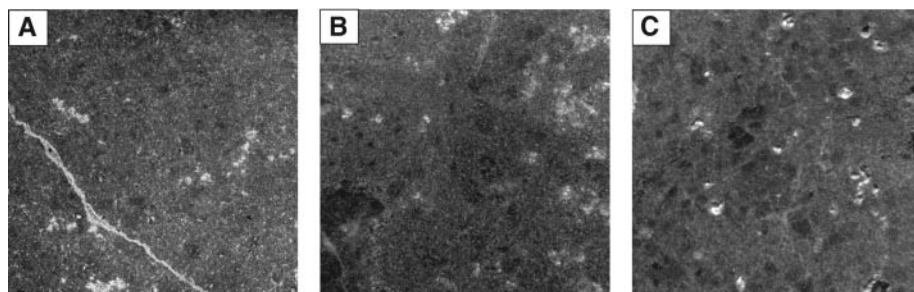


Fig. 3. MI subframes of rock interiors comparing the textures of (A) Adirondack (image no. 2M133914681EFF2232P2959M2M1, slightly contrast-enhanced to correct for shadowing), (B) Humphrey (image no. 2M131690279EFF1155P2939M2M1), and (C) Mazatzal (image no. 2M129468509EFF0327P2943M2M1). All three rocks contain dark megacrysts, presumably olivine. Images are $\sim 1.2\text{ cm}$ wide.

¹Department of Earth and Planetary Sciences, University of Tennessee, Knoxville, TN 37996–1410, USA.

²Department of Earth and Planetary Sciences, Washington University, St. Louis, MO 63130–4899, USA.

³Department of Astronomy, Cornell University, Ithaca, NY 14853–6801, USA. ⁴Jet Propulsion Laboratory, California Institute of Technology, Pasadena, CA 91109–8099, USA.

⁵NASA Ames Research Center, Moffett Field, CA 94035–1000, USA. ⁶Department of Geological Sciences, Arizona State University, Tempe, AZ 85287–6305, USA.

⁷Lockheed Martin Corporation, Littleton, CO 80127, USA. ⁸New Mexico Museum of Natural History and Science, Albuquerque, NM 87104, USA.

⁹Max Planck Institut für Chemie, D-55099 Mainz, Germany. ¹⁰Honeybee Robotics, New York, NY 10012, USA.

¹¹National Air and Space Museum, Smithsonian Institution, Washington, DC 20560, USA. ¹²U.S. Geological Survey, Flagstaff, AZ 86001–1698, USA.

¹³Institut für Anorganische und Analytische Chemie, Johannes Gutenberg–Universität, Mainz, Germany. ¹⁴Department of Geosciences, State University of New York, Stony Brook, NY 11794–2100, USA.

¹⁵NASA Johnson Space Center, Houston, TX 77058, USA. ¹⁶Companhia Vale do Rio Doce, 29090–900 Vitória, ES, Brazil.

¹⁷Department of Geosciences, State University of New York, Stony Brook, NY 11794–2100, USA.

¹⁸Department of Geosciences, State University of New York, Stony Brook, NY 11794–2100, USA.

¹⁹Department of Geosciences, State University of New York, Stony Brook, NY 11794–2100, USA.

*To whom correspondence should be addressed, E-mail: mcsween@utk.edu

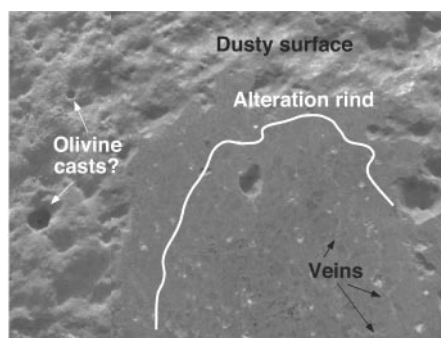


Fig. 2. Composite MI image (no. 2M131690279EFF1155P2939M2M1) of an oblique RAT grind into Humphrey, illustrating its natural surface containing hexagonal casts, a brushed surface, an inferred alteration rind, and an interior containing tiny, irregular veins. The view is $\sim 3\text{ cm}$ wide.

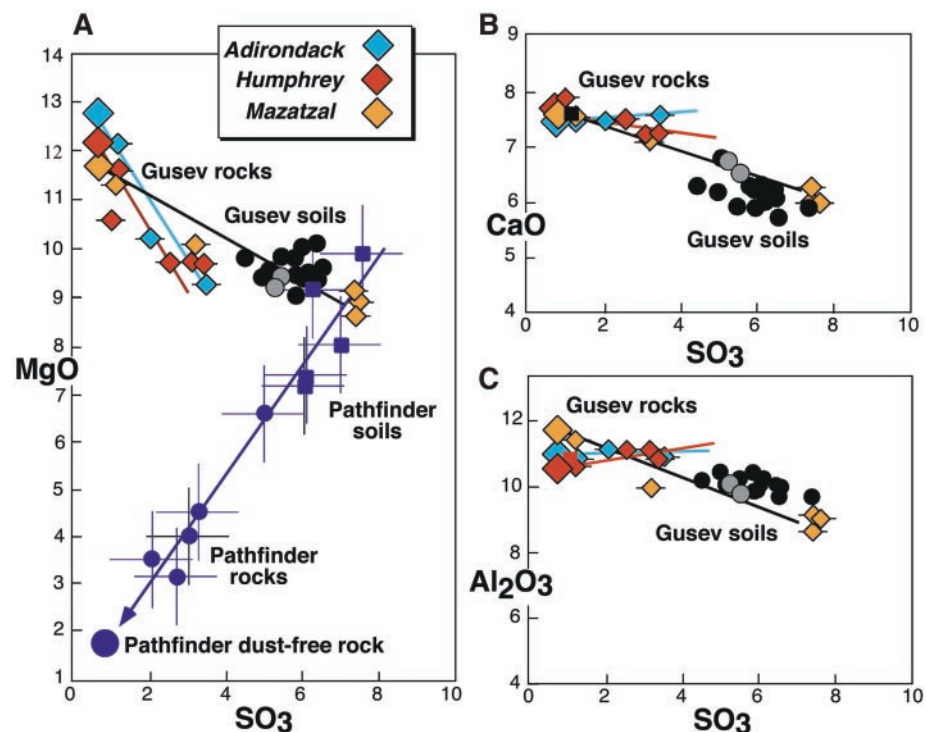


Fig. 4. APXS chemical variations (wt % oxides) among rocks (blue, red, and yellow diamonds), soil-coated rocks (gray circles), and soils (black circles) from Gusev: (A) MgO–SO₃, also showing data for Mars Pathfinder rocks and soils (dark blue symbols) (12); (B) CaO–SO₃; and (C) Al₂O₃–SO₃. Calculated compositions (Table 1) of uncoated rocks (large diamonds) are extrapolated from trends defined by analysis of natural, brushed, and abraded rocks (small diamonds), which decrease progressively in SO₃. Absolute statistical errors (17) are illustrated only for rock analyses.

Some vesicles and vugs filled with similar white material may be amygdules. The presence of multiple surface coatings and cross-cutting, fracture-filling materials may suggest alteration by several generations of fluids, although surface coatings might have formed by weathering reactions without a condensed fluid phase. The energy used in grinding a unit volume of all three rocks was lower than for a reference unaltered terrestrial basalt (7), supporting observations that these rocks are partly altered. MI images of the abraded interiors of all three rocks reveal dark megacrysts (Fig. 3), presumably olivine (9), in an aphanitic groundmass. The images are suitable for point counting, giving 9%, 25%, and 9% (by volume) megacrysts in Adirondack, Humphrey, and Mazatzal, respectively, and 13% and 14% patches of light-colored material in Adirondack and Mazatzal. Bright materials plus megacrysts sum to the same value in the three rocks, perhaps suggesting the light-toned materials are alteration products of olivine. However, the megacrysts and presumed alteration materials are distributed heterogeneously, so point counts on other areas might give differing results.

Least squares fitting of Mössbauer spectra for Adirondack, Humphrey, and Mazatzal (10) indicates the presence of olivine, pyroxene, and magnetite. Because Mössbauer spectra generally sample a greater depth (50 to 200 μm) than do other spectra (<100 μm), a weak ferric doublet may be associated with alteration rinds or veins. Estimated molar Fe^{2+}/Fe (total) values for abraded rocks are 0.84, 0.84, and 0.90 ± 0.04 for Adirondack, Humphrey, and Mazatzal, respectively (10), similar to values for terrestrial basalts (0.85 to 0.90).

Alpha Particle X-ray Spectrometer (APXS) chemical variations (11) among the undisturbed, brushed, and abraded surfaces of Adirondack, Humphrey, and Mazatzal are illustrated in Fig. 4. Martian soils (12) are enriched in SO_3 compared to martian meteorites and Pathfinder rocks. The natural, brushed, and abraded rock compositions do not define a mixing line with Gusev soils, as do dust-covered Mars Pathfinder rocks and soils (Fig. 4A) (13). Distinct trends for Adirondack, Humphrey, and Mazatzal indicate that coatings on Gusev rocks have compositions different from the local regolith. By extrapolating trends defined by the natural, brushed, and abraded compositions for each rock to 0.3 weight percent (wt %) residual S (0.75 wt % SO_3), the average sulfur abundance in basaltic martian meteorites (13), the compositions of rock end members can be calculated (Table 1). Except for variations in the relative proportions of Fe oxides, the derived chemical compositions of the interiors of Adirondack, Humphrey, and Mazatzal are indistinguishable.

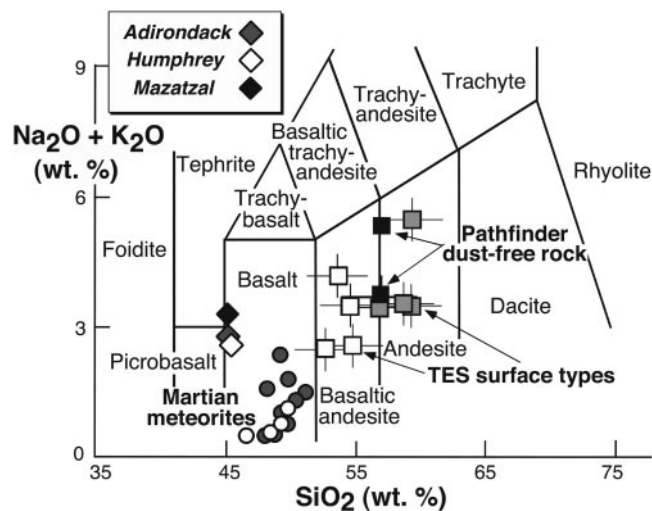


Fig. 5. Chemical classification diagram for volcanic rocks (14), comparing the compositions of Adirondack, Humphrey, and Mazatzal (diamonds) with those of basaltic martian meteorites (gray circles are shergottites, and open circles are nakhlites), two calibrations of the Mars Pathfinder dust-free rock (black squares), and MGS-TES surface types (open and gray squares are surface types 1 and 2, respectively). Data are from McSween *et al.* (16).

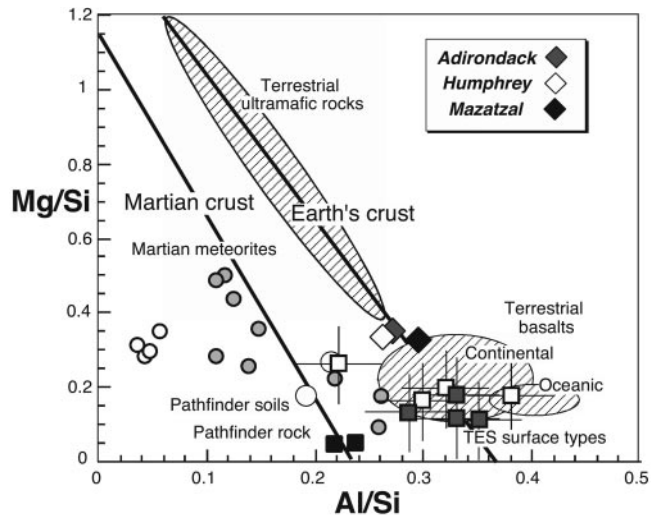
Table 1. Extrapolated chemical compositions of Gusev rocks and calculated norms. Rock end-member compositions were calculated by subtracting from the deepest RAT-abraded APXS composition enough of the average of brushed and natural surface APXS analyses reported by Gellert *et al.* (11) (20%, 25%, and 7% for Adirondack, Humphrey, and Mazatzal, respectively) to reduce residual S to 0.3 wt % (13). Iron was partitioned between FeO and Fe_2O_3 on the basis of Mössbauer measurements (10) of molar Fe^{2+}/Fe (total) of 0.84, 0.84, and 0.90 for the three rocks, respectively. Rock compositions were recast into mineralogy by calculating norms, after removing S as FeS and Cl as NaCl. Plag, plagioclase; Or, orthoclase; Ab, albite; An, anorthite; Ne, nepheline; Di, diopside; Hy, hypersthene; Ol, olivine; Fo, forsterite; Fa, fayalite; Cr, chromite; Mt, magnetite; Ilm, ilmenite; Ap, apatite.

Composition	Adirondack	Humphrey	Mazatzal
<i>Oxides (wt %)</i>			
SiO ₂	45.4	46.1	45.7
TiO ₂	0.46	0.52	0.48
Al ₂ O ₃	10.9	10.6	11.7
Fe ₂ O ₃	3.02	2.99	1.80
Cr ₂ O ₃	0.60	0.59	0.56
FeO	15.2	15.3	15.6
MnO	0.41	0.39	0.36
MgO	12.8	12.2	11.6
CaO	7.49	7.70	7.71
Na ₂ O	2.79	2.59	3.30
K ₂ O	0.06	0.06	0.07
P ₂ O ₅	0.52	0.56	0.70
S	0.30	0.30	0.30
Cl	0.09	0.11	0.15
Total	100.0	100.0	100.1
<i>Norms (wt %)</i>			
Plag	40.6 (An ₄₃)	38.9 (An ₄₅)	44.1 (An ₄₀)
Or	0.4	0.4	0.4
Ab	22.9	21.1	26.2
An	17.3	17.5	17.5
Ne	0	0	(0.32)
Di	13.5	14.0	13.3
Hy	6.3	12.9	0
Ol	31.1 (Fo ₅₅)	26.1 (Fo ₅₂)	35.0 (Fo ₅₁)
Fo	17.1	13.7	17.8
Fa	14.0	12.4	17.2
Cr	0.9	0.9	0.8
Mt	4.4	4.3	2.6
Ilm	0.9	1.0	0.9
Ap	1.2	1.3	1.7

On an alkali-silica classification diagram for volcanic rocks (14), Gusev rocks plot near the junction between basalt, picrobasalt, and tephrite (Fig. 5). In the Irvine-Baragar classification (15), these

rocks are basalts. This olivine-rich composition is substantially more primitive than those of basaltic martian meteorites, Pathfinder rocks, and the calculated compositions of TES surface types 1 and 2 (16).

Fig. 6. Mg/Si versus Al/Si variations in Gusev rocks compared with other martian materials (19). Symbols are as in Fig. 5.



Gusev basalts apparently experienced very little fractionation.

Rock compositions can be recast into mineralogy by calculating norms (Table 1). The norms are dominated by olivine, pyroxene, and plagioclase, with accessory magnetite, chromite, ilmenite, and apatite. A tiny amount of nepheline in the Mazatzal norm is probably an artifact of the assigned Mössbauer oxidation state; if calculated with Fe^{2+}/Fe (total) similar to the other rocks, Mazatzal would also be hypersthene normative. The normative olivine compositions (Fo51–55) are less magnesian and plagioclase compositions (An40–45) are more sodic than comparable minerals in terrestrial basalts, but are consistent with olivine and plagioclase compositions in martian meteorites (17). This suggests that the mineralogy of martian meteorites may be generally characteristic of igneous rocks on Mars. Normative mineralogy conforms to mineralogic constraints from Mössbauer, Pancam, and Mini-TES spectra.

An estimate of the equilibrium crystallization sequence of magmas having these compositions, calculated from MELTS simulation (18) at low pressure and an oxidation state buffered by quartz-fayalite-magnetite, indicates early appearance of Cr-spinel and olivine, followed by plagioclase, clinopyroxene, orthopyroxene, and phosphate. The prediction of olivine as an abundant, early

crystallizing phase suggests the megacrysts seen in MI images are olivine phenocrysts. We cannot rule out the possibility that olivine in these rocks is cumulus or xenocrystic. However, the similar chemical compositions of the rocks, despite their textural differences, suggest that they were melts. Low Ni/Cr weight ratios (~ 0.04) for these rocks (11) may also argue against the addition of olivine (which has high Ni/Cr). We have also considered the possibility that these rocks were impact melts containing unmelted mineral clasts, but no breccias have been observed at Gusev and the rocks' low Ni/Cr ratios suggest no substantial added meteoritic component.

The regional geologic context for these basalts is unclear. There are no obvious effusive centers within Gusev crater, and flows into the crater from the only nearby volcano (Apolinaris Patera) are not apparent. Whatever their source, Gusev rocks do not plot on the low Al/Si trend defined by martian meteorites (Fig. 6) (19). The high Al contents of Gusev basalts could reflect melting of an ancient, relatively undepleted mantle (16), but low contents of incompatible K and P and the presence of normative olivine plus hypersthene suggest a depleted mantle source. These picritic lavas are the least fractionated materials so far encountered on

Mars. The rocks at Gusev expand the known range of volcanic compositions and the recognized extent of crustal heterogeneity. Despite orbital interpretations that large amounts of surface water shaped the Gusev landscape, the alteration of these rocks required only limited amounts of groundwater.

References and Notes

- Names have been assigned to aerographic features by the Mars Exploration Rover (MER) team for planning and operations purposes. The names are not formally recognized by the International Astronomical Union.
- J. A. Grant *et al.*, *Science*, **305**, 807 (2004).
- S. W. Squyres *et al.*, *Science*, **305**, 794 (2004).
- J. F. Bell III *et al.*, *Science*, **305**, 800 (2004).
- T. M. Hoefen *et al.*, *Science*, **302**, 627 (2003).
- P. R. Christensen *et al.*, *Science*, **305**, 837 (2004).
- R. E. Arvidson *et al.*, *Science*, **305**, 821 (2004).
- K. E. Herkenhoff *et al.*, *Science*, **305**, 824 (2004).
- Euhedral olivine crystals commonly have hexagonal shapes like the pits in Fig. 2, although megacrysts in rock interiors are anhedral.
- R. V. Morris *et al.*, *Science*, **305**, 833 (2004).
- R. Gellert *et al.*, *Science*, **305**, 829 (2004).
- The term martian soil is used here to denote any loose unconsolidated materials that can be distinguished from rocks, bedrock, or strongly cohesive sediments. No implication of the presence or absence of organic materials or living matter is intended.
- J. Brückner, G. Dreibus, R. Rieder, H. Wänke, *J. Geophys. Res.*, **108**, 8094 (2003).
- M. J. LeBas, R. W. LeMaitre, A. Streckeisen, B. Zanettin, *J. Petrol.*, **27**, 745 (1986).
- T. N. Irvine, W. R. A. Barragar, *Canad. J. Earth Sci.*, **8**, 523 (1971).
- H. Y. McSween, T. L. Grove, M. B. Wyatt, *J. Geophys. Res.*, **108**, 5135 (2003).
- H. Y. McSween, A. H. Treiman, in *Planetary Materials*, J. Papike, Ed. (Mineralogical Society of America, Washington, DC, 1998), chap. 6.
- M. S. Ghiorso, R. O. Sack, *Contrib. Mineral. Petrol.*, **119**, 197 (1995).
- H. Wänke, J. Brückner, G. Dreibus, R. Rieder, I. Ryabchikov, *Space Sci. Rev.*, **96**, 317 (2001).
- A martian solar day has a mean period of 24 hours 39 min 35.244 s and is referred to as a sol to distinguish this from a roughly 3%-shorter solar day on Earth. A martian sidereal day, as measured with respect to the fixed stars, is 24 hours 37 min 22.663 s, as compared with 23 hours 56 min 04.0905 s for Earth. See <http://www.giss.nasa.gov/tools/mars24/> for more information.
- Funding for Athena science team members was provided by NASA contracts through Cornell and the Jet Propulsion Laboratory.

Plates Referenced in Article

www.sciencemag.org/cgi/content/full/305/5685/842/DC1
Plates 9 to 11

3 May 2004; accepted 23 June 2004